A Femoral Clamp to Reduce Soft Tissue Artefact: Accuracy and Reliability in Measuring Three-Dimensional Knee Kinematics During Gait

Ding, Ziyun[1]
Department of Bioengineering
Imperial College London London,
SW7 2AZ United Kingdom
z.ding@imperial.ac.uk

Güdel, Manuela
Department of Bioengineering
Imperial College London London,
SW7 2AZ United Kingdom
manuela.g@bluewin.ch

Smith, Samuel H L
Department of Bioengineering
Imperial College London
London, SW7 2AZ United Kingdom
Samuel.Smith781@mod.gov.uk

Ademefun, Richard A
Department of Bioengineering
Imperial College London London,
SW7 2AZ United Kingdom
richardademefun@yahoo.co.uk

Bull, Anthony M J
Department of Bioengineering
Imperial College London London,
SW7 2AZ United Kingdom
a.bull@imperial.ac.uk

ABSTRACT

The accurate measurement of full six degrees-of-freedom (DOFs) knee joint kinematics is prohibited by soft tissue artifact (STA), which remains the greatest source of error. The purpose of this study was to present and assess a new femoral clamp to reduce STA at the thigh. It was hypothesised that the device can preserve the natural knee joint kinematics pattern and outperform a conventional marker mounted rigid cluster during gait. Six healthy subjects were asked to walk barefoot on level ground with a cluster marker set (cluster gait) followed by a cluster-clamp-merged marker set (clamp gait) and their kinematics was measured using the cluster method in cluster gait and the cluster and clamp methods simultaneously in clamp gait. Two operators performed the gait measurement. A six DOFs knee joint model was developed to enable comparison with the gold standard knee joint kinematics measured using a dual fluoroscopic imaging technique. One-dimensional paired t-tests were used to compare the knee joint kinematics waveforms between cluster gait and clamp gait. The accuracy was assessed in terms of the root mean square error, coefficient of determination and Bland-Altman plots. Inter-operator reliability was assessed using the intra-class correlation coefficient. The result showed that the femoral clamp did not change the walking speed and knee joint kinematics waveforms. Additionally, clamp gait reduced the rotation and translation errors in the transverse plane and improved the interoperator reliability when compared to the rigid cluster method, suggesting a more accurate and reliable measurement of knee joint kinematics.

INTRODUCTION

The knee joint is one of the most complicated synovial joints [1] that primarily moves in flexion/extension and external/internal rotation [2]. Coupled motions, due to the articular geometry and the rolling and sliding of the knee as the flexion and extension moments introduce shear forces, result in abduction/adduction and anterior/posterior translation [1–3]. These coupled motions are important in pathologies and injuries, such as knee osteoarthritis [4,5] and ligament rupture [6–9]. Therefore, in order to monitor and evaluate such conditions, the ability to measure the full six degrees-of-freedom (6DOFs), or three dimensional (3D), knee joint kinematics is required [10–13].

Although technologies exist to measure bone motion directly [14–20], these are clinically impractical due to a combination of invasiveness (for example, pins inserted to the bones, or ionising radiation), cost (advanced imaging), limited field of view (imaging), time (scanning, imaging segmentation and registration), and ethics. Therefore, other methods are preferred clinically, which infer motion of the underlying bones from the movement of overlying soft tissue. These include, for example, electromagnetic motion tracking [21], and marker-based [22] or markerless optical motion tracking [23,24], and include techniques to minimise the effect of soft tissue artefact (STA), which is the relative movement of soft tissue to the underlying bones due to inertial effects, skin stretching/sliding, and muscle contractions [25–27]. At the knee joint, STA particularly affects the measurement of subtle movements such as abduction/adduction, external/internal rotation, anterior/posterior and lateral/medial translations: the tracking errors between the surface markers and the underlying bone can be up 40 mm at the thigh and 15 mm at the shank [28–31], resulting in rotation errors of up to 20° and translation errors of 20 mm in both the frontal and transverse planes. For planes of motion other than the sagittal plane, STA remains the main limitation of these measurement technologies.

STA can be corrected mathematically through the application of optimisation techniques, including the least squares method [32–35] and the point cluster technique [36,37]. Although these techniques provide encouraging results they can only compensate for the inter-marker movement, which is a minor component of STA [30,38]. Global optimisation techniques have been developed which use underlying knee joint models that include kinematic constraints to limit STA [39,40]. These constraints, to either a 1 DOF hinge or a 3 DOFs sphere, may in fact increase the error due to over-simplification of the complex knee joint [38]. Additionally, they are too restrictive in clinical practice for the study of knee pathologies that, by definition, include motion in the other DOFs [27].

To measure knee joint motion both the shank and the thigh need to be tracked accurately. Shank STA is very small compared to STA at the thigh [26] and therefore the focus of this study is to better measure knee joint kinematics by devising a technique to measure thigh motion. The approach taken is to develop a device to physically attach to the thigh, tracking the femur. Such attachment systems have been designed previously [41,42], for example, the KneeKG system, that has been shown to have an accuracy of 2.5° in rotation and 2.5 mm in translation during non-weightbearing knee flexion/extension [1,41]. As knee joint kinematics is activity dependent [22,27], these results cannot be generalised for weightbearing activities, such as gait. Another variable that needs to be considered is whether such a device would change the natural kinematics pattern during gait. The purposes of the study were twofold: first, to present a new femoral device to reduce STA at the thigh; and second, to assess its performance in tracking knee joint kinematics during overground walking. The hypothesis of the study was that the device can preserve the natural knee joint kinematics pattern and outperform a conventional marker mounted rigid cluster in accuracy and reliability during gait.

METHODS

The femoral clamp design and fabrication

The device functions on two key principles, where the first is that the femoral epicondyles are very close to the surface of the skin and clamping at the epicondyles will reduce errors in all planes of motion, except flexion/extension which will cause twisting and shear on the surface that is difficult to control. The flexion/extension motion between surface and bone is then resisted by a stabilising bar that straps along the anterior aspect of the thigh. However, the thigh soft tissue can rotate around the bone. A fixed bar would then transmit this rotation to the epicondyles and result in the device separating from its attachment points. Therefore, the stabilising bar is attached to the clamp with a rotational bearing that permits axial rotation without changing the flexion/extension position of the bar.

The femoral clamp consists of two femoral pads, a femoral arch, a stabilizing bar and the distal and proximal Velcro straps (Fig.1). The 40.0-mm-diameter, 8.0-mm-thick circular femoral pads are 3D-printed (Ultimaker 2, Ultimaker B.V., Geldermalsen, Netherlands) using PLA (PolyLactic Acid). They are placed over the medial and lateral femoral epicondyles and are interconnected over the front of the knee via an 8.0-mm-thick femoral arch, made of moulded Polycaprolactone (PCL), designed to have an appropriate stiffness to apply a compressive force to the epicondyles. To further minimise the movement between the femoral pads and the underlying bone, they are attached posteriorly by a distal Velcro strap. The stabilizing bar consists of a proximal part and a distal part angled 160° to the proximal part. The proximal part rests on the anterior aspect of the thigh, restricting the rotation of the device in the sagittal plane. The distal part inserts into the femoral arch through a pivot bearing. The mass of the whole device is 63 g.

Insert figure 1

Validation experiment

Six healthy subjects (three male and three female; age 31.4 ± 4.0 years; height 1.76 ± 0.10 m; mass 74.3 ± 16.8 kg; body mass index 23.8 ± 3.5 kg/m^2) with no self-reported lower limb musculoskeletal pain or impairments were recruited. Institutional ethics approval and informed consent were obtained. Subjects were asked to walk barefoot at a self-selected speed on level ground with a cluster-based marker set (cluster gait) followed by a clusterclamp-merged marker set (clamp gait) on their pelvises and right legs. Knee joint motion was measured using the cluster method in cluster gait and the cluster and clamp methods simultaneously in clamp gait. In the cluster-based marker set, reflective markers were placed on the anterior/posterior superior iliac spine, medial/lateral femoral epicondyles, medial/lateral malleoli, second/fifth metatarsal head, and lateral and posterior calcaneus. Additionally, two clusters of three markers were placed onto the lateral and frontal aspects of the thigh and shank (Fig. 2) [43]. Three walking trials were recorded for cluster gait, as well as a standing reference trial of subjects standing in a neutral position before the walking trials. In clamp gait the markers on the medial/lateral femoral epicondyles were removed and five markers were placed on the clamp (Fig.1d). Once the clamp was aligned and stable, subjects were given several practice trials (including walking and standing up from a chair) to familiarise themselves with the device. Similar to cluster gait, three walking trials and a standing reference trial were recorded. The protocol was performed by two separate operators with experience in palpating bony landmarks. The order of the operators was randomised. Following completion of the protocol the first time, the whole marker set was removed, and subjects were given a break; then the second operator repeated the identical protocol. Marker trajectories were measured with a 10-camera optical motion capture system (Vicon Motion Systems Ltd, Oxford, UK, 100 Hz). Measured kinematics was initially processed in Vicon Nexus (V2.6.1), including labelling, gap filling and heel strikedetection (using the vertical component of the posterior calcaneus marker [44]), and then lower-pass filtered using a fourth-order, zero-lag Butterworth filter with a cut-off frequency of 6 Hz [45] in MATLAB (The MathWorks Inc., USA).

Insert Figure 2

Knee model

The knee is described with full six DOFs with the anatomical geometry scaled from an MR-based musculoskeletal (MSK) model (female, 43 years, 1.84 m, 78 kg [46]), implemented in an open source musculoskeletal modelling software, FreeBody (v2.1, [47,48]). To enable the comparison with knee joint kinematics in the literature measured using the gold standard dual fluoroscopic imaging technique [49], the coordinate system of the thigh and shank and rotations and translations at the knee are defined as follows (see Fig.3): the thigh origin is the midpoint between the medial and lateral femoral epicondyles, the superior - inferior (SI) - axis points from the thigh origin to the hip joint centre (centre of a sphere fitted to the femoral head), the temporary lateral - medial (tempLM) - axis points from the medial to lateral femoral epicondyle, the anterior - posterior (AP) - axis is the cross product of the SI and tempLM axes, pointing anteriorly and the LM - axis is the cross product of the AP and SI axes, pointing laterally; the shank origin is the midpoint between the centres of two circles fitting the medial and lateral plateaus separately, the SI - axis points from the midpoint of medial and lateral malleoli to the shank origin, the tempLM - axis connects the centres of plateau circles, the (AP) - axis is the cross product of the SI and tempLM axes, pointing anteriorly and the LM - axis is the cross product of the AP and SI axes, pointing laterally. The bony landmarks on the anterior/posterior superior iliac spine from the MSK model and the same landmarks from the standing reference trial were used to construct the hip joint centre and similarly, the landmarks on the femoral epicondyles and malleoli from the MSK model and from the reference trial were used to construct the shank origin, based on the method described by Soderkvist and Wedin [32, 48]. Knee rotations are calculated as the orientation of the shank with respect to the thigh, resolving the Cardan angles in the sequence of flexion/extension, abduction/adduction and external/internal rotation [2]; knee translations are calculated as the displacement of the thigh origin with respect to the shank origin, represented in the shank LCS [8]. The location and orientation of the thigh and shank segments are determined based on the method described by Horn et al.[35]: for the thigh segment constructed using three markers from the thigh cluster in the cluster method and three markers from the femoral arch in the clamp method; for the shank segment using three markers from the shank cluster in both methods. All markers are visible during the analysed gait cycles. The resulting knee kinematics was normalised to 100% of the gait cycle with 101 sample points.

Insert Figure 3

Data analysis

To test whether the device changes the walking pattern, walking speed and knee joint kinematics were compared. Walking speed, was calculated as the distance of the posterior calcaneus marker in a gait cycle divided by time and averaged over three walking trials for both cluster and clamp gait. Waveforms of knee joint kinematics in cluster gait were compared with waveforms in clamp gait as measured using the cluster method. Onedimensional (1D) two-tail paired t-tests (α = 0.05) based on the methodology of statistical parametric mapping (SPM, [50]) were conducted using "SPM1D", an open-source package for SPM, written in MATLAB (http://www.spm1d.org/index.html, [38]). This computes the Fstatistics (SPM {t}) and critical threshold (t*): a statistical difference is detected if SPM {t} exceeds the threshold.

For clamp gait, knee joint kinematics as measured using the cluster method and the clamp method were assessed in terms of the accuracy and inter-operator reliability and their differences were compared using the non-parametric Wilcoxon signed rank test in SPSS (Version 24.0, IBM Corp., USA, α = 0.05). Eleven data points during stance (0-60% of gait, starting from 0% of gait with 6 percentage point intervals) were calculated from the ensemble average knee joint kinematics over three walking trials. The accuracy when compared to the gold standard knee joint kinematics [49] was assessed in terms of the root mean square error (RMSE), coefficient of determination (r^2) and Bland-Altman plots (including the bias and confidence interval: 1.96 standard deviation). The inter-operator reliability was assessed using ICCs (intra-class correlation coefficients, two-way randomeffects, absolute agreement model in SPSS [51]), where values of less than 0.5, between 0.5 and 0.75, between 0.75 and 0.90, and greater than 0.90 are indicative of poor, moderate, good, and excellent reproducibility, respectively [52]. ICCs were calculated for eleven data points (starting from 0% of gait with 10 percentage point intervals) as well as the range of motion (ROM) and peaks during gait and expressed as mean over six subjects. Figure 4 shows the flowchart of the data analysis in the study.

Insert Figure 4

RESULTS

There was no significant difference in walking speed (1.20 m/s vs 1.22 m/s, respectively, p = 0.753) or knee joint kinematics waveforms (p > 0.05; Fig.5) between cluster gait and clamp gait.

Insert figure 5

The clamp method produced smaller errors in external/internal rotation, anterior/posterior and lateral/medial translations when compared to the cluster method as evaluated by the reductions in the range of Bland-Altman bias ([0.2, 4.3] vs. [-4.6, 6.9] ° in external/internal rotation; [-2.9, 13.0] vs. [-3.4, 13.7] mm in anterior/posterior translation; and [-4.7, 1.2] vs. [-7.3, 1.9] mm in lateral/medial translation) and confidence interval ([-6.1, 11.3] vs. [-8.7, 12.5] ° in external/internal rotation; [-2.6, 13.4] vs. [-6.2, 15.4] mm in anterior/posterior translation; and [-9.2, 2.5] vs. [-16.8, 7.9] mm in lateral/medial translation) as well as the mean RMSEs (3.3 ± 0.8 vs. 4.6 ± 0.9 ° in external/internal rotation; 7.1 ± 4.5 vs. 8.1 ± 4.6 mm in anterior/posterior translation; and 2.9 ± 1.4 vs. 5.8 ± 2.4 mm in lateral/medial translation). When compared to the gold standard data from the literature, the device is a better fit to the kinematics in the transverse plane, as assessed by the greater r^2 (0.60 ± 0.06 vs. 0.20 ± 0.02 in external/internal rotation; 0.61 ± 0.15 vs. 0.40 ± 0.21 in anterior/posterior translation; and 0.63 ± 0.18 vs. 0.28 ± 0.06 mm in lateral/medial translation, p = 0.031).

Insert figure 6 and TABLE 1.

For 13 data points of interest during clamp gait, ICCs ranged from 0.50 to 0.96 in the cluster method and ranged from 0.61 to 0.98 in the clamp method. When compared to the cluster method, the device improved the inter-operator reliability in abduction/adduction (0.84 vs. 0.70, p=0.001), external/internal rotation (0.84 vs. 0.72, p=0.017), anterior/posterior (0.84 vs. 0.70, p=0.004), and lateral/medial (0.88 vs. 0.76, p=0.001) translations.

Insert TABLE 2

DISCUSSION

The purpose of this study was to present and assess a femoral device to reduce STA, which is a major limitation in the measurement of full 6DOFs of knee joint kinematics. The first key finding was that our proposed device did not change the walking speed and the natural knee kinematics pattern of subjects, enabling the use of this device in gait analysis.

Previous studies comparing knee joint kinematics measured concurrently during gait from surface markers and using the fluoroscopic imaging found the rotation errors to be up to 7.5° [53] and translation errors up to 7 mm [54] in the non-sagittal plane. In particular, external/internal rotation and lateral/medial translation displayed the largest errors in functional activities [53,54]. The errors reported from the cluster method were in the same range as these prior studies in the non-sagittal plane. For the new clamp device there was a decrease in measured knee translation and rotation errors in the transverse plane and the results were a better fit to the gold standard measurements from the literature. This suggests that there is a reduction in the relative transverse movement between the clamp and the femur compared to the cluster-based technique, resulting in an improvement in the measurement reliability. As there was a reduction in errors in tracking the femur, this might result in an improvement in the measurement of hip joint kinematics, although this wasn't assessed in this study.

The new device still showed considerable knee superior/inferior translation and this amount of translation is not seen in direct measures using bone pins and imaging [25, 37]. This DOF also had the lowest ICC. Therefore, the method should not be used to comment on absolute values and patterns of superior/inferior translation at the knee.

The intra-operator reliability of the custom-made cluster used in the study has been reported previously [43]. Other researchers also investigated inter-operator reliability using the cluster method for knee rotations [55]. Although the use of different reliability index impedes the direct comparison, similar findings have been obtained: the reliability was low in the non-sagittal plane with the lowest value for knee abduction/adduction. The use of the clamp provided a more reliable measure of knee joint kinematics in the non-sagittal plane, which may partly be due to the reduced STA. Furthermore, the femoral clamp appears to have less uncertainty in reinstallation than the thigh cluster, as it will only stabilise on the thigh when it is properly positioned. However, the mean and the range of ICCs for knee rotations were slightly lower in this study when compared to other similar clamps (i.e., the KneeKG with ICCs ranging from 0.89 to 0.94, compared to 0.84 to 0.90 here [57]). The mass of the clamp made from PCL presented here (63 g) is significantly less than other similar clamps (with mass ranging from 125 g [1] to 180 g [42]). Therefore, it is expected that, an improved fixation of the stabilising bar with the femoral clamp may further reduce the effect of gravity and improve its reliability; this is being investigated.

There were some limitations to this study. First, sizing of this device could be improved and even customised through using rapid manufacturing techniques. The current device was only suited for medium-sized knees and additional sizes with different arch width would be required for very large or very small knees, as the fit of the arch to the femoral epicondyles is a key component of the device's tracking capability. Secondly, as an assessment of the accuracy, the gold standard knee joint kinematics from the literature was collected for a different subject group walking on a treadmill at a preferred reduced walking speed. Simultaneous data collection with fluoroscopy was not possible in this study and this may explain the considerable errors in knee flexion/extension from both methods. Furthermore, this study was limited to young, healthy subjects and so future work should focus on using subjects that reflect a clinical population.

In conclusion, the results partially support the hypothesis that for self-selected walking, our proposed device is more accurate and reliable in measuring knee joint kinematics than a conventional rigid cluster-based method in the transverse plane.

ACKNOWLEDGEMENT

This work of Z. Ding was conducted under the auspices of the Royal British Legion Centre for Blast Injury Studies at Imperial College London. Z. Ding would like to acknowledge the financial support of the Royal British Legion.

NOMENCLATURE

DOFs	degrees-of-freedom
ICC	Intra-class correlation coefficient
PLA	poly lactic acid
PCL	polycaprolactone
RMSE	root mean square error
ROM	range of motion
SPM	statistical parametric mapping
STA	soft tissue artefact

REFERENCES

[1] Ganjikia, S., Duval, N., Yahia, L., and De Guise, J., 2000, “Three-Dimensional Knee Analyzer Validation by Simple Fluoroscopic Study,” Knee, **7**(4), pp. 221–231. DOI: 10.1016/S0968-0160(00)00063-6

[2] Grood, E. S., and Suntay, W. J., 1983, “A Joint Coordinate System for the Clinical Description of Three-Dimensional Motions: Application to the Knee,” J. Biomech. Eng., **105**(2), p. 136. DOI: 10.1115/1.3138397

[3] Bull, A. M. J., and Amis, A. A, 1998, “Knee Joint Motion: Description and Measurement,” Proc. Inst. Mech. Eng. H., **212**(5), pp. 357–372. DOI: 10.1243/0954411981534132

[4] Manal, K., Gardinier, E., Buchanan, T. S., and Snyder-Mackler, L., 2015, “A More Informed Evaluation of Medial Compartment Loading: The Combined Use of the Knee Adduction and Flexor Moments,” Osteoarthr. Cartil., **23**(7), pp. 1107–1111. DOI: 10.1016/j.joca.2015.02.779

[5] Landry, S. C., McKean, K. A., Hubley-Kozey, C. L., Stanish, W. D., and Deluzio, K. J., 2007, “Knee Biomechanics of Moderate OA Patients Measured during Gait at a Self-Selected and Fast Walking Speed,” J. Biomech., **40**(8), pp. 1754–1761. DOI: 10.1016/j.jbiomech.2006.08.010

[6] Dennis, D. A., Mahfouz, M. R., Komistek, R. D., and Hoff, W., 2005, “In Vivo Determination of Normal and Anterior Cruciate Ligament-Deficient Knee Kinematics,” J. Biomech., **38**(2), pp. 241–253. DOI: 10.1016/j.jbiomech.2004.02.042

[7] Defrate, L. E., Papannagari, R., Gill, T. J., Moses, J. M., Pathare, N. P., and Li, G., 2006, “The 6 Degrees of Freedom Kinematics of the Knee after Anterior Cruciate Ligament Deficiency: An in Vivo Imaging Analysis,” Am. J. Sports Med., **34**(8), pp. 1240–1246. DOI: 10.1177/0363546506287299

[8] Li, J. S., Tsai, T. Y., Felson, D. T., Li, G., and Lewis, C. L., 2017, “Six Degree-of-Freedom Knee Joint Kinematics in Obese Individuals with Knee Pain during Gait,” PLoS One, **12**(3), pp. 1–11. DOI: 10.1371/journal.pone.0174663

[9] Georgoulis, A. D., Papadonikolakis, A., Papageorgiou, C. D., Mitsou, A., and Stergiou, N., 2003, “Three-Dimensional Tibiofemoral Kinematics of the Anterior Cruciate LigamentDeficient and Reconstructed Knee during Walking.,” Am. J. Sports Med., **31**(1), pp. 75–79. DOI: 10.1177/03635465030310012401

[10] Azmi, N. L., Ding, Z., Xu, R., and Bull, A. M. J., 2018, “Activation of Biceps Femoris Long Head Reduces Tibiofemoral Anterior Shear Force and Tibial Internal Rotation Torque in Healthy Subjects,” Plos One, **13**(1), pp. 1–13. DOI: 10.1371/journal.pone.0190672

[11] Zingde, S. M., Leszko, F., Sharma, A., Mahfouz, M. R., Komistek, R. D., and Dennis, D. A., 2014, “In Vivo Determination of Cam-Post Engagement in Fixed and Mobile-Bearing TKA Knee,” Clin. Orthop. Relat. Res., **472**(1), pp. 254–262. DOI:10.1007/s11999-013-3257-3

[12] Komistek, R. D., Mahfouz, M. R., Bertin, K. C., Rosenberg, A., and Kennedy, W., 2008, “In Vivo Determination of Total Knee Arthroplasty Kinematics. A Multicenter Analysis of an Asymmetrical Posterior Cruciate Retaining Total Knee Arthroplasty,” J. Arthroplasty, **23**(1), pp. 41–50. DOI: 10.1016/j.arth.2007.01.016

[13] Kang, K.T., Koh, Y.G., Son, J., Jung, M., Oh, S., Kim, S.J., and Kim, S.H., 2018, “Biomechanical Influence of Deficient Posterolateral Corner Structures on Knee Joint Kinematics: A Computational Study,” J. Orthop. Res., **36**(8), pp. 1–8. DOI: 10.1002/jor.23871

[14] Biswas, D., Bible, J. E., Bohan, M., Simpson, A. K., Whang, P. G., and Grauer, J. N., 2009, “Radiation Exposure from Musculoskeletal Computerized Tomographic Scans,” J. Bone. Joint. Surg. Am., **91**(8), pp. 1882–1889. DOI: 10.2106/JBJS.H.01199

[15] Lin, C.C, Zhang S, Frahm J, Lu T.W., Hsu C.Y., Shih T.F., 2013, “A Slice-to-Volume Registration Method Based on Real-Time Magnetic Resonance Imaging for Measuring Three-Dimensional Kinematics of the Knee,” Med.Phys., **40**(10), p. 102302. DOI: 10.1118/1.4820369.

[16] Lu, T., Tsai, T., Kuo, M., Hsu, H., and Chen, H., 2008, “In Vivo Three-Dimensional Kinematics of the Normal Knee during Active Extension under Unloaded and Loaded Conditions Using Single-Plane Fluoroscopy,” Med. Eng. Phys., 30, pp. 1004–1012. DOI: 10.1016/j.medengphy.2008.03.001

[17] Ramsey, D. K., and Wretenberg, P. F., 1999, “Biomechanics of the Knee: Methodological Considerations in the in Vivo Kinematic Analysis of the Tibiofemoral and Patellofemoral Joint,” Clin. Biomech., **14**(9), pp. 595–611. DOI:10.1016/S02680033(99)00015-7.

[18] Leardini, A., Chiari, L., Della, U., and Cappozzo, A., 2005, “Human Movement Analysis Using Stereophotogrammetry Part 3. Soft Tissue Artifact Assessment and Compensation,” Gait Posture., **21**(2), pp. 212–225. DOi:10.1016/j.gaitpost.2004.05.002

[19] Souza, R. B., Draper, C. E., Fredericson, M., and Powers, C. M., 2010, “Femur Rotation and Patellofemoral Joint Kinematics: A Weight-Bearing Magnetic Resonance Imaging Analysis,” J. Orthop. Sport. Phys. Ther., **40**(5), pp. 277–285. DOI:10.2519/jospt.2010.3215.

[20] Lafortune, M. A., Cavanagh, P. R., Sommer, H. J., and Kalenak, A., 1992, “ThreeDimensional Kinematics of the Human Knee during Walking,” J. Biomech., **25**(4), pp. 347– 357. DOI:10.1016/0021-9290(92)90254-X.

[21] Alam, M., Bull, A. M. J., Thomas, R. deW, and Amis, A. A, 2013, “A Clinical Device for Measuring Internal-External Rotational Laxity of the Knee.,” Am. J. Sports Med., **41**(1), pp. 87–94. DOI: 10.1177/0363546512469874

[22] Cappozzo, A., Catani, F., Leardini, A., Benedetti, M. G., and Croce, U. D., 1996, “Position and Orientation in Space of Bones during Movement: Experimental Artefacts,” Clin. Biomech., **11**(2), pp. 90–100. DOI:10.1016/0268-0033(95)00046-1

[23] Castelli, A., Paolini, G., Cereatti, A., and Croce, U. Della, 2015, “A 2D Markerless Gait Analysis Methodology: Validation on Healthy Subjects,” Comput. Math. Methods Med., DOI: 10.1155/2015/186780

[24] Grigg, J., Haakonssen, E., Rathbone, E., Orr, R., and Keogh, J. W. L., 2018, “The Validity and Intra-Tester Reliability of Markerless Motion Capture to Analyse Kinematics of the BMX Supercross Gate Start,” Sport. Biomech., **17**(3), pp. 383–401. DOI: 10.1080/14763141.2017.1353129.

[25] Kim, H. J., Fernandez, J. W., Akbarshahi, M., Walter, J. P., Fregly, B. J., and Pandy, M. G., 2009, “Evaluation of Predicted Knee-Joint Muscle Forces during Gait Using an Instrumented Knee Implant,” J. Orthop. Res., **27**(10), pp. 1326–1331. DOI:10.1002/jor.20876

[26] Clément, J., Dumas, R., Hagemeister, N., and de Guise, J. A., 2015, “Soft Tissue Artifact Compensation in Knee Kinematics by Multi-Body Optimization: Performance of Subject-Specific Knee Joint Models,” J. Biomech., **48**(14), pp. 3796–3802. DOI: 10.1016/j.jbiomech.2015.09.040.

[27] Cappello, A., Stagni, R., Fantozzi, S., and Leardini, A., 2005, “Soft Tissue Artifact Compensation in Knee Kinematics by Double Anatomical Landmark Calibration: Performance of a Novel Method during Selected Motor Tasks,” IEEE Trans. Biomed. Eng., **52**(6), pp. 992–998. DOI:10.1109/TBME.2005.846728.

[28] Benoit, D. L., Ramsey, D. K., Lamontagne, M., Xu, L., Wretenberg, P., and Renström, P., 2006, "Effect of Skin Movement Artifact on Knee Kinematics during Gait and Cutting Motions Measured in Vivo," Gait Posture, **24**(2), pp. 152–164. DOI: 10.1016/j.gaitpost.2005.04.012

[29] Lucchetti, L., Cappozzo, A., Cappello, A., and Croce, U. Della, 1998, "Skin Movement Artefact Assessment and Compensation in the Estimation of Knee-Joint Kinematics," J. Biomech. **31**(11), pp. 977–984. DOI:10.1016/S0021-9290(98)00083-9.

[30] Benoit, D. L., Damsgaard, M., and Andersen, M. S., 2015, "Surface Marker Cluster Translation, Rotation, Scaling and Deformation: Their Contribution to Soft Tissue Artefact and Impact on Knee Joint Kinematics," J. Biomech., **48**(10), pp. 2124–2129. DOI: 10.1016/j.jbiomech.2015.02.050.

[31] Sati, M., de Guise J.A., Larouche, S., and Drouin, G., 1995, "Quantitative assessment of skin-bone movement at the knee," Knee., 3, pp. 121-138. DOI: https://doi.org/10.1016/0968-0160(96)00210-4

[32] Soderkvist, I., and Wedin, P. A., 1993, "Determining the Movements of the Skeleton Using Well-Configured Markers," J. Biomech., **26**(12), pp. 1473–1477. DOI:10.1016/00219290(93)90098-Y.

[33] Carman, A. B., and Milburn, P. D., 2006, "Determining Rigid Body Transformation Parameters from Ill-Conditioned Spatial Marker Co-Ordinates," J. Biomech., **39**(10), pp. 1778–1786. DOI:10.1016/j.jbiomech.2005.05.028.

[34] Spoor, C. W., and Veldpaus, F. E., 1980, "Rigid Body Motion Calculated from Spatial Co-Ordinates of Markers," J. Biomech., **13**(4), pp. 391–393. DOI: 10.1016/00219290(80)90020-2

[35] Horn, B. K. P., 1987, "Closed-Form Solution of Absolute Orientation Using Unit Quaternions," J. Opt. Soc. Am. A, 4, pp. 629. DOI:10.1364/JOSAA.4.000629

[36] Andriacchi, T. P., Alexander, E. J., Toney, M. K., Dyrby, C., and Sum, J., 1998, "A Point Cluster Method for In Vivo Motion Analysis: Applied to a Study of Knee Kinematics," J. Biomech. Eng., **120**(6), p. 743. DOI: 10.1115/1.2834888.

[37] Alexander, E. J., and Andriacchi, T. P., 2001, "Correcting for Deformation in SkinBased Marker Systems," J. Biomech., **34**(3), pp. 355–361. DOI:10.1016/S00219290(00)00192-5.

[38] Potvin, B. M., Shourijeh, M. S., Smale, K. B., and Benoit, D. L., 2017, “A Practical Solution to Reduce Soft Tissue Artifact Error at the Knee Using Adaptive Kinematic Constraints,” J. Biomech., **62**, pp. 124–131. DOI: 10.1016/j.jbiomech.2017.02.006.

[39] Andersen, M. S., Benoit, D. L., Damsgaard, M., Ramsey, D. K., and Rasmussen, J., 2010, “Do Kinematic Models Reduce the Effects of Soft Tissue Artefacts in Skin Marker-Based Motion Analysis? An in Vivo Study of Knee Kinematics,” J. Biomech., **43**(2), pp. 268–273. DOI:10.1016/j.jbiomech.2009.08.034.

[40] Liu, T.W., and O’Connor, J. J, 1999, “Bone position estimation from skin marker coordinates using global optimisation with joint constraints,” J.Biomech., **32**(2), pp. 129-134. DOI: 10.1016/S0021-9290(98)00158-4.

[41] Sati, M., De Guise, J. A., Larouche, S., and Drouin, G., 1996, “Improving in Vivo Knee Kinematic Measurements: Application to Prosthetic Ligament Analysis,” Knee, **3**(4), pp. 179– 190. DOI: 10.1016/S0968-0160(96)00209-8.

[42] Houck, J., Yack, H. J., and Cuddeford, T., 2004, “Validity and Comparisons of Tibiofemoral Orientations and Displacement Using a Femoral Tracking Device during Early to Mid Stance of Walking,” Gait Posture, **19**(1), pp. 76–84. DOI:10.1016/S0966-6362(03)00033-X.

[43] Duffell, L. D., Hope, N., and McGregor, A. H., 2014, “Comparison of Kinematic and Kinetic Parameters Calculated Using a Cluster-Based Model and Vicon’s Plug-in Gait,” Proc. Inst. Mech. Eng. H., **228**(2), pp. 206–10. DOI:10.1177/0954411913518747.

[44] Di Marco, R., Rossi, S., Racic, V., Cappa, P., and Mazzà, C., 2016, “Concurrent repeatability and reproducibility analyses of four marker placement protocols for the footankle complex,” J. Biomech., **49**(14), pp.3168-3176. doi: 10.1016/j.jbiomech.2016.07.041.

[45] Yu, B., Gabriel, D., Noble, L., and An, KN. 1999 “Estimate of the optimum cutoff frequency for the Butterworth low-pass digital filter,” J. Appl. Biomech. 15, pp.318–329. DOI: 10.1123/jab.15.3.318

[46] Ding, Z., Tsang, C. K., Nolte, D., Kedgley, A. E., and Bull, A. M. J., 2019, “Improving Musculoskeletal Model Scaling Using an Anatomical Atlas: The Importance of Gender and Anthropometric Similarity to Quantify Joint Reaction Forces,” IEEE Trans. Biomed. Eng., DOI: 10.1109/TBME.2019.2905956.

[47] Cleather, D. J., and Bull, A. M. J., 2015, “The Development of a Musculoskeletal Model of the Lower Limb: Introducing FREEBODY,” R.Soc.Open Sci, 2:140449.

[48] Ding, Z., Nolte, D., Kit Tsang, C., Cleather, D. J., Kedgley, A. E., and Bull, A. M. J., 2016, “In Vivo Knee Contact Force Prediction Using Patient-Specific Musculoskeletal Geometry in a Segment-Based Computational Model,” J. Biomech. Eng., **138**(2), p. 021018.
DOI:10.1115/1.4032412

[49] Kozanek, M., Hosseini, A., Liu, F., Van de Velde, S. K., Gill, T. J., Rubash, H. E., and Li, G., 2009, “Tibiofemoral Kinematics and Condylar Motion during the Stance Phase of Gait,” J. Biomech., **42**(12), pp. 1877–1884. DOI:10.1016/j.jbiomech.2009.05.003

[50] Pataky, T. C., 2012, “One-Dimensional Statistical Parametric Mapping in Python,” Comput. Methods Biomech. Biomed. Engin., **15**(3), pp. 295–301. DOI: 10.1080/10255842.2010.527837

[51] Koo, T.K., and Li, M.Y., 2016, “Guideline of Selecting and Reporting Intraclass Correlation Coefficients for Reliability Research,” J. Chiropr. Med., 15(2), pp.155-163. DOI:
10.1016/j.jcm.2016.02.012

[52] Manal, K., McClay, I., Stanhope, S., Richards, J., and Galinat, B., 2000, “Comparison of Surface Mounted Markers and Attachment Methods in Estimating Tibial Rotations during Walking: An In Vivo Study,” Gait Posture, **11**(1), pp. 38–45. DOI: 10.1016/S09666362(99)00042-9.

[53] Akbarshahi M., Schache AG., Fernandez JW., Baker R., Banks S., and Pandy MG., 2010, “Non-invasive Assessment of Soft-tissue Artifact and its Effect on Knee Joint Kinematics during Functional Activity,” J Biomech, **43**(7), pp. 1292-1301. DOI: 10.1016/j.jbiomech.2010.01.002.

[54] Richard V., Cappozzo A., Dumas R., 2017, “Comparative Assessment of Knee Joint Models Used in Multi-body Kinematics Optimisation for Soft Tissue Artefact Compensation,” J Biomech, 62, pp. 95-101. DOI: 10.1016/j.jbiomech.2017.01.030.

[55] Besier, T.F., Sturnieks, D.L., Alderson, J.A., Lloyd, D.G., 2003, “Repeatability of Gait Data Using a Functional Hip Joint Centre and A Mean Helical Knee Axis,” J Biomech, 36, pp. 1159-1168.DOI: 10.1016/s0021-9290(03)00087-3.

[56] Labbe DR., Hagemeister N., Tremblay M., and de Guise J., 2008, “Reliability of A Method for Analyzing Three-dimensional Knee Kinematics during Gait,” Gait Posture., **28**(1), pp. 170-174. DOI: 10.1016/j.gaitpost.2007.11.002

Figure Captions List

Fig. 1

The femoral clamp (a) and its lateral (b) and frontal (c) view on the thigh segment; the lateral femoral pad is placed at the posterior aspect of the lateral epicondyle and the medial femoral pad is placed at the superior aspect of the medial epicondyle; (d) the soft tissue can move around the axis of rotation without affecting the clamp attachments.

Fig.2

Marker placement for the cluster-based gait methodology. Markers are placed on: right anterior superior iliac spine (RASIS), left anterior superior iliac spine (LASIS), right posterior superior iliac spine (RPSIS), left posterior superior iliac spine (LPSIS), medial femoral epicondyle (MFE), lateral femoral epicondyle (LFE), medial malleolus (MM), lateral malleolus (LM), second metatarsal head (MTHII), fifth metatarsal head (MTHV), lateral calcaneus (LCAL) and posterior calcaneus (PCAL).

Fig.3

Local coordinate systems of the thigh and shank segments: the lateral – medial (LM) axis is the cross product of the anterior – posterior (AP) and superior – inferior (SI) axes, pointing laterally. The red dots represent the origins; the black dots represent the medial/lateral femoral epicondyles; and the white dots represent the centres of two circles fitted to the medial and lateral plateaus.

Fig. 4 Data analysis flowchart.

Fig. 5 Comparison of mean (solid line) and standard deviation (shaded area) knee joint kinematics waveforms between cluster gait and clamp gait for one representative subject. Knee flexion(+)/extension(-), abduction(+)/adduction(-), external(+)/internal(-) rotation, anterior(+)/posterior(-), superior(+)/inferior(-) and lateral(+)/medial(-) translations are measured using the cluster method. The horizontal dashed line indicates the critical thresholds (t* = 31.757, α = 0.05). Regions of the gait cycle for which SPM {t} exceeded the critical threshold are considered as statistically significant differences.

Fig. 6 Knee joint kinematics (mean in solid line and standard deviation in shaded area) measured using the cluster method and the clamp method during clamp gait (left panel) for one representative subject, compared to the literature [44]. The differences in eleven data points digitised from the ensemble average kinematics during stance (0-60% of gait, starting from 0% of gait with 6 percentage point intervals) in comparison with the literature are represented in the Bland-Altman plots (right panel) with the corresponding root mean square error (RMSE) and coefficient of determination (r^2).

Table Caption List

Table 1 The accuracy of knee joint kinematics as measured using the cluster method and the clamp method during clamp gait, in comparison with the literature data [44]. Bland-Altman bias (B) and confidence interval (CI) are expressed as range; room mean square error (RMSE) and coefficient of determination (r^2) are expressed as mean (standard deviation) across six subjects. The non-parametric Wilcoxon signed rank test is performed to compare the differences in RMSE and r^2between the two methods.

Table 2 Inter-operator reliability to measure knee joint kinematics using the cluster method in comparison with the clamp method during clamp gait. The intra-class correlation coefficients (ICCs)are calculated for the range of motion (ROM), peak, eleven points during the gait cycle (starting from 0% of gait with 10 percentage point intervals) and expressed as mean across six subjects. The non-parametric Wilcoxon signed rank test is performed to compare the differences in ICCs between the two methods.

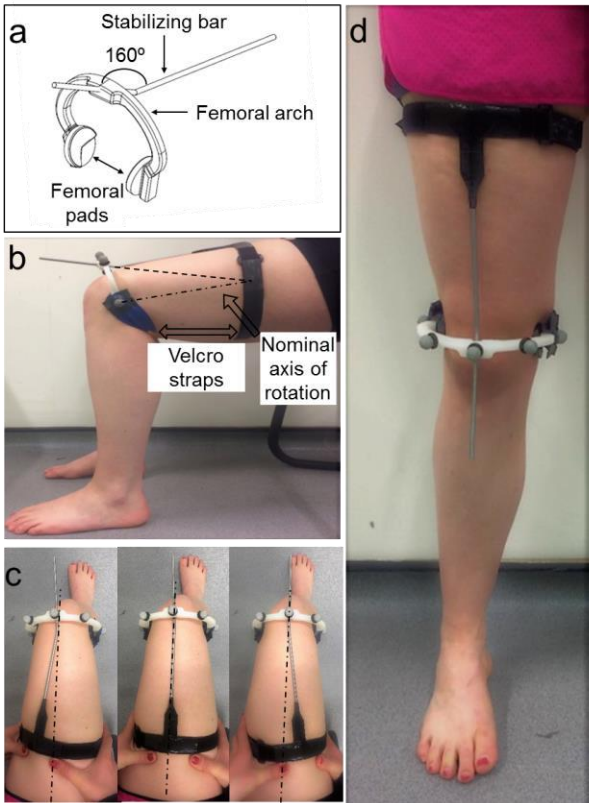

Fig.1. The femoral clamp (a) and its lateral (b) and frontal (d) view on the thigh segment; the lateral femoral pad is placed at the posterior aspect of the lateral epicondyle and the medial femoral pad is placed at the superior aspect of the medial epicondyle; (c) the soft tissue can move around the axis of rotation without affecting the clamp attachments.

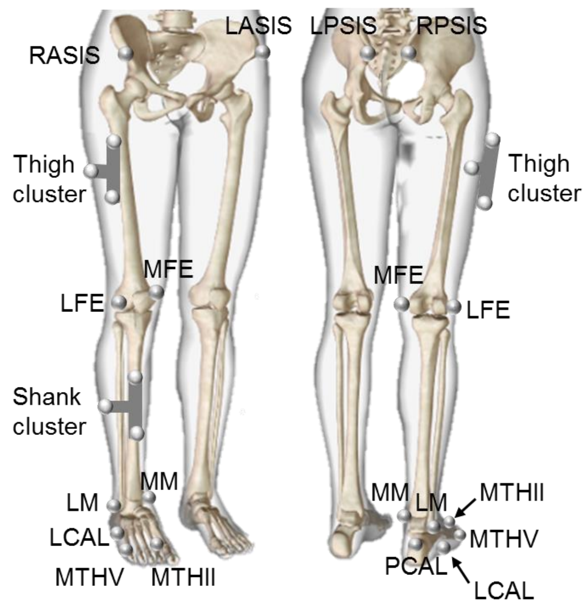

Fig.2 Marker placement for the cluster-based gait methodology. Markers are placed on: right anterior superior iliac spine (RASIS), left anterior superior iliac spine (LASIS), right posterior superior iliac spine (RPSIS), left posterior superior iliac spine (LPSIS), medial femoral epicondyle (MFE), lateral femoral epicondyle (LFE), medial malleolus (MM), lateral malleolus (LM), second metatarsal head (MTHII), fifth metatarsal head (MTHV), lateral calcaneus (LCAL) and posterior calcaneus (PCAL).

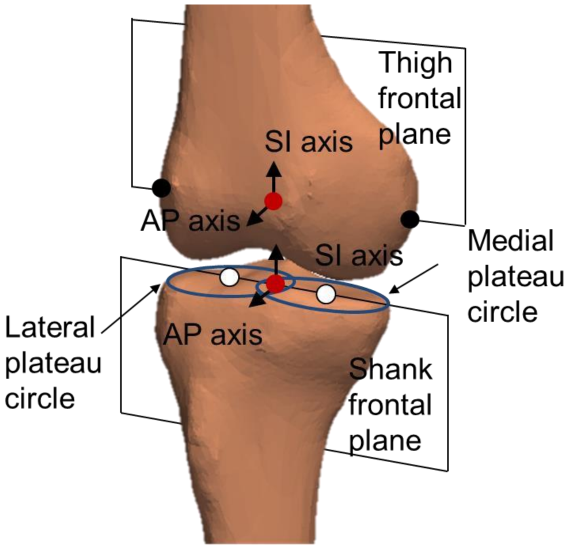

Fig.3 Local coordinate systems of the thigh and shank segments: the lateral – medial (LM) axis is the cross product of the anterior – posterior (AP) and superior – inferior (SI) axes, pointing laterally. The red dots represent the origins of the thigh and the shank; the black dots represent the medial/lateral femoral epicondyles; and the white dots represent the centres of two circles fitted to the medial and lateral plateaus.

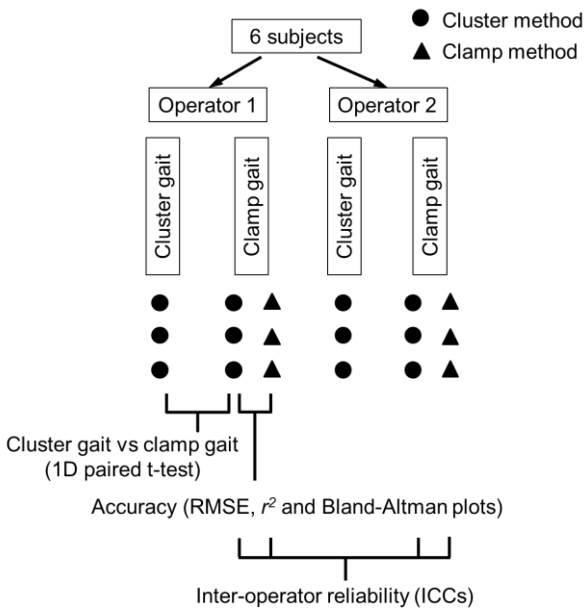

Fig.4 Data analysis flowchart.

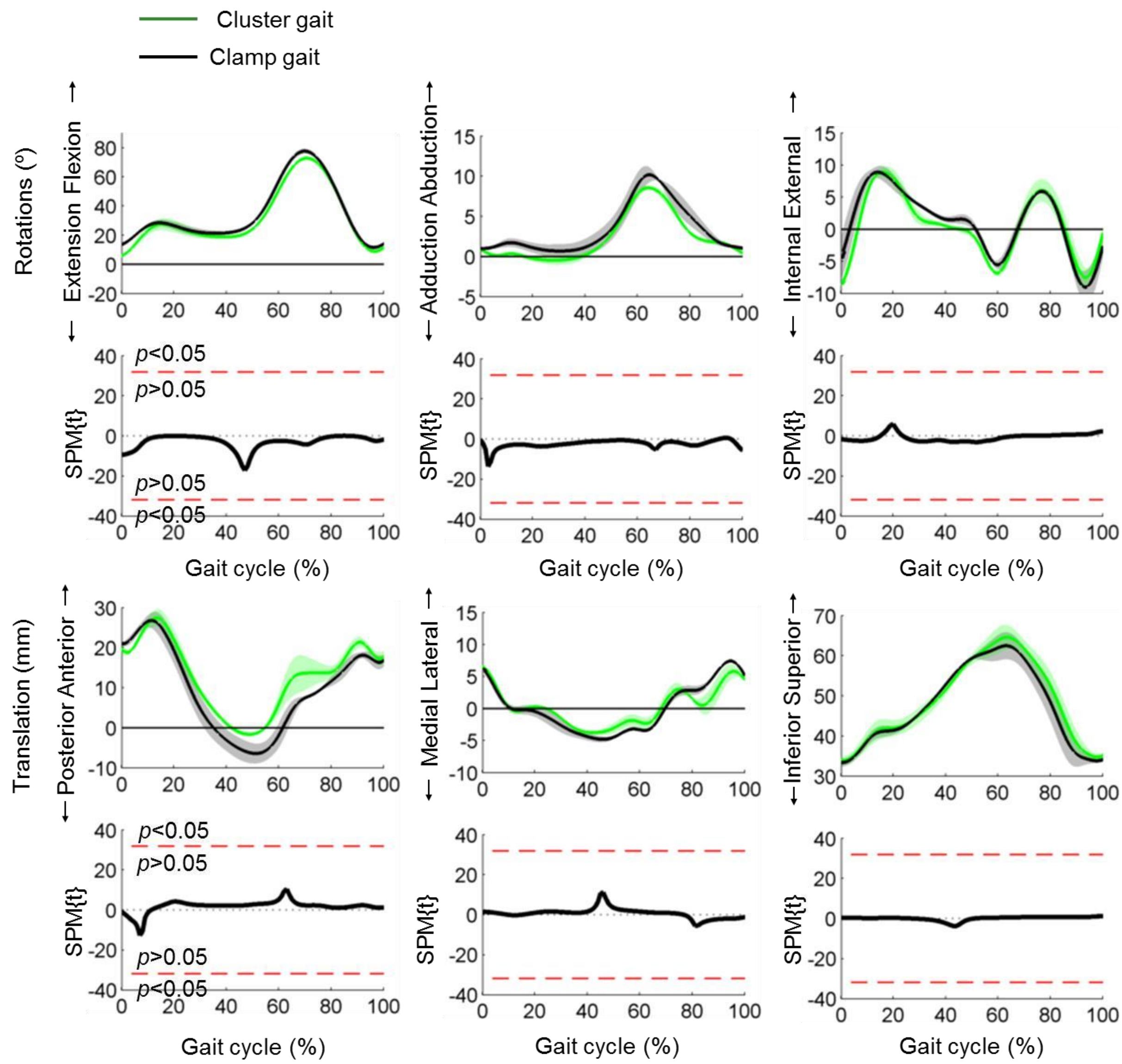

Fig.5. Comparison of mean (solid line) and standard deviation (shaded area) knee joint kinematics waveforms between cluster gait and clamp gait for one representative subject. Knee flexion(+)/extension(-), abduction(+)/adduction(-), external(+)/internal(-) rotation, anterior(+)/posterior(-), superior(+)/inferior(-) and lateral(+)/medial(-) translations are measured using the cluster method. The horizontal dashed line indicates the critical thresholds (t* = 31.757, α = 0.05). Regions of the gait cycle for which SPM {t} exceeded the critical threshold are considered as statistically significant differences.

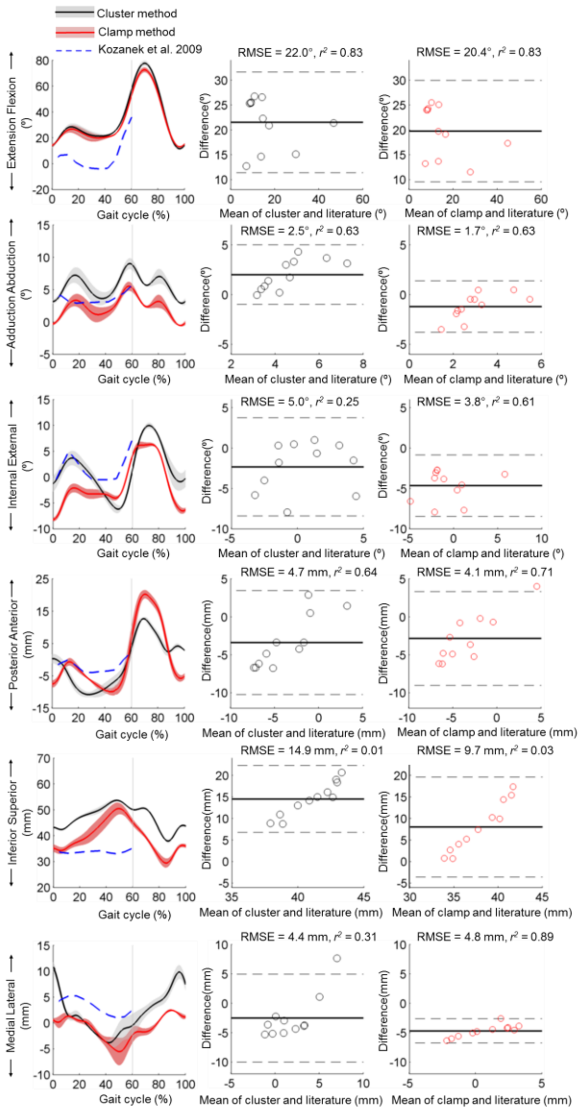

Fig.6. Knee joint kinematics (mean in solid line and standard deviation in shaded area) measured using the cluster method and the clamp method during clamp gait (left panel) for one representative subject, compared to the literature [44]. The differences in eleven data points digitised from the ensemble average kinematics during stance (0-60% of gait, starting from 0% of gait with 6 percentage point intervals) in comparison with the literature are represented in the Bland-Altman plots (right panel) with the corresponding root mean square error (RMSE) and coefficient of determination (r^2).

Table 1. The accuracy of knee joint kinematics as measured using the l cluster method and the clamp method during clamp gait, in comparison with the literature data [44]. Bland-Altman bias (B) and confidence interval (CI) are expressed as range; room mean square error (RMSE) and coefficient of determination (r^2) are expressed as mean (standard deviation) across six subjects. The non-parametric Wilcoxon signed rank test is performed to compare the differences in RMSE and r^2between the two methods.

	Fle/ext (º)				Abd/add (º)				Ext/int (º)			
	B	CI	RMSE	r^2	B	CI	RMSE	r^2	B	CI	RMSE	r^2
cluster	-2.1,21.5	-12.3, 32.1	11.2(6.1)	0.85(0.03)	-4.0,3.2	-8.4,7.2	2.9(1.2)	0.61(0.14)	-4.8, 6.9	-8.7,12.5	4.6(0.9)	0.20(0.02)
clamp	-0.5,19.8	-8.6,30.6	11.5(5.7)	0.84(0.02)	-4.2,1.2	-6.8,5.3	2.6(0.8)	0.57(0.08)	0.2,4.3	-6.1,11.3	3.3(0.8)	0.60(0.06)
p-value			0.688	0.688			0.688	0.219			0.219	0.031*
	Ant/pos (mm)				Sup/inf (mm)				Lat/med (mm)			
	B	CI	RMSE	r^2	B	CI	RMSE	r^2	B	CI	RMSE	r^2
cluster	-3.4,13.7	-6.2, 15.4	8.1(4.6)	0.40(0.21)	2.9,15.5	-5.3,32.3	12.9(4.9)	0.02(0.01)	-7.3, 1.9	-16.8,7.9	5.8(2.4)	0.28(0.06)
clamp	-2.9,13.0	-2.6,13.4	7.1(4.5)	0.61(0.15)	-3.6,10.7	-15.7,37.0	11.2(5.4)	0.01(0.01)	-4.7,1.2	-9.2,2.5	2.9(1.4)	0.63(0.18)
p-value			0.688	0.031*			0.688	1.000			0.319	0.031*

Fle/ext = flexion/extension, Abd/add = abduction/adduction, Ext/int = external/internal rotation, Ant/pos = anterior/posterior translation,

Sup/inf = superior/inferior translation, Lat/med = lateral/medial translation. * indicates significantly different ($p \leq 0.05$).

Table 2. Inter-operator reliability to measure knee joint kinematics using the cluster method in comparison with the clamp method during clamp

gait. The intra-class correlation coefficients (ICCs) are calculated for the range of motion (ROM), peak, eleven points during the gait cycle (starting from 0% of gait with 10 percentage point intervals) and expressed as mean across six subjects. The non-parametric Wilcoxon signed rank test was performed to compare the differences in ICCs between the two methods.

	ICC											
	Fle/ext		Abd/add		Ext/int		Ant/pos		Sup/inf		Lat/med	
	Cluster	Clamp	Cluster	Clamp	Cluster	Clamp	Cluster	Clamp	Cluster	Clamp	Cluster	Clamp
ROM	0.96	0.92	0.79	0.81	0.82	0.94	0.66	0.83	0.85	0.94	0.73	0.88
Peak	0.94	0.93	0.80	0.80	0.62	0.84	0.74	0.76	0.59	0.92	0.71	0.90
0% Gait	0.91	0.88	0.70	0.79	0.55	0.90	0.72	0.87	0.65	0.78	0.75	0.79
10% Gait	0.87	0.86	0.72	0.76	0.78	0.87	0.74	0.81	0.67	0.78	0.73	0.93
20% Gait	0.88	0.81	0.67	0.90	0.72	0.78	0.79	0.94	0.74	0.90	0.85	0.98
30% Gait	0.94	0.95	0.63	0.82	0.88	0.80	0.78	0.90	0.92	0.80	0.77	0.86
40% Gait	0.88	0.94	0.71	0.97	0.83	0.92	0.85	0.84	0.90	0.94	0.70	0.88
50% Gait	0.92	0.87	0.69	0.80	0.82	0.80	0.83	0.90	0.60	0.92	0.78	0.77
60% Gait	0.94	0.93	0.77	0.94	0.81	0.88	0.68	0.75	0.76	0.94	0.73	0.96
70% Gait	0.94	0.90	0.61	0.77	0.54	0.80	0.50	0.84	0.69	0.62	0.67	0.84
80% Gait	0.91	0.87	0.69	0.89	0.59	0.78	0.50	0.83	0.63	0.61	0.81	0.88
90% Gait	0.96	0.96	0.52	0.85	0.70	0.85	0.52	0.92	0.77	0.91	0.76	0.86
100% Gait	0.80	0.83	0.77	0.78	0.68	0.76	0.82	0.71	0.85	0.78	0.85	0.94
Mean	0.91	0.90	0.70	0.84	0.72	0.84	0.70	0.84	0.74	0.83	0.76	0.88
p-value	0.245		0.001*		0.017*		0.004*		0.180		0.001*	

Fle/ext = flexion/extension, Abd/add = abduction/adduction, Ext/int = external/ internal rotation, Ant/pos = anterior/posterior translation, Sup/inf = superior/inferior translation, Lat/med = lateral/medial translation. *indicates significantly different ($p \leq 0.05$).